Journal of Environmental Management 360 (2024) 121160

Contents lists available at ScienceDirect

Journal of Environmental Management

journal homepage: www.elsevier.com/locate/jenvman

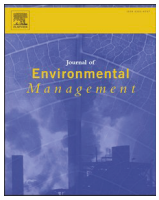

Research article

Amino-modified upcycled biochar achieves selective chromium removal in complex aqueous matrices

Kenneth Flores [a,*], Diego F. Gonzalez [b], Helia M. Morales [b,c], Arnulfo Mar [b], Sergi Garcia-Segura [a], Jorge L. Gardea-Torresdey [d], Jason G. Parsons [e,**]

[a] Nanosystems Engineering Research Center for Nanotechnology-Enabled Water Treatment, School of Sustainable Engineering and the Built Environment, Arizona State University, Tempe, AZ, 85287-3005, USA
[b] School of Integrative Biological and Chemical Sciences University of Texas Rio Grande Valley, 1 West University Blvd., Brownsville, TX, 78521, USA
[c] Escuela de Ingeniería y Ciencias, Tecnologico de Monterrey, Av E Garza Sada # 2501, Monterrey, 64849, Mexico
[d] Department of Chemistry & Biochemistry and Environmental Science and Engineering, University of Texas at El Paso, El Paso, TX, 79968, USA
[e] School of Earth Environmental, and Marine Science, University of Texas Rio Grande Valley, 1 West University Blvd., Brownsville, TX, 78521, USA

ARTICLE INFO

Keywords:
Biochar
Amino-modified
Cr(VI)
Cr(III)
Adsorption
Selectivity
Agricultural waste

ABSTRACT

Chromium pollution of groundwater sources is a growing global issue, which correlates with various anthropogenic activities. Remediation of both the Cr(VI) and Cr(III), via adsorption technologies, has been championed in recent years due to ease of use, minimal energy requirements, and the potential to serve as a highly sustainable remediation technology. In the present study, a biochar sorbent sourced from pineapple skins, allowed for the upcycling of agricultural waste into water purification technology. The biochar material was chemically modified, through a green amination method, to produce an efficient and selective adsorbent for the removal of both Cr(VI) and Cr(III) from complex aqueous matrices. From FTIR analysis it was evident that the chemical modification introduced new C–N and N–H bonds observed in the modified biochar along with a depletion of N–O and C–H bonds found in the pristine biochar. The amino modified biochar was found to spontaneously adsorb both forms of chromium at room temperature, with binding capacities of 46.5 mg/g of Cr(VI) and 27.1 mg/g of Cr(III). Interference studies, conducted in complex matrices, showed no change in adsorption capacity for Cr(VI) in matrices containing up to 3,000× the concentration of interfering ions. Finally, Cr(III) removal was synergized to 100% adsorption at interfering ions concentrations up to 330× of the analyte, which were suppressed at higher interference concentrations. Considering such performance, the amino modified biochar achieved selective removal for both forms of chromium, showing great potential for utilization in complex chromium pollution sources.

1. Introduction

Heavy metal pollution in ground water continues to rise globally aggravated by anthropogenic activities (Liu et al., 2023a). Chromium is one of the most toxic metal ions; its presence in water poses severe implications to both environmental and human health (Mallik et al., 2022). The continual increase in chromium pollution is directly related to industrial and mining activity. Industrial uses for chromium include production of steels and sophisticated alloys, wood and paper processing, paint and dye production, and various chrome plating processes (Tumolo et al., 2020a; Zhitkovich, 2011). Chromium species as heavy metal pollutants are non-biodegradable, which results in long term pollution of soil and water sources (Sharma et al., 2022). Chromium in aqueous solutions may exist primarily as either Cr(VI) or Cr(III). Chronic ingestion of Cr(VI) can result in grave effects for human health; these include DNA damage, chromosomal aberration, and cancer development (N. Chen et al., 2021a; Tumolo et al., 2020b). The Cr(VI) species presents higher risks to both human and environmental health via greater solubility, mobility, and toxicity (Zhitkovich, 2011). In contrast, Cr(III) may be considered the less harmful form; however, this species may still serve as a potential reservoir for the hexavalent species, as Cr (III) can be naturally oxidized in the environment (Varadharajan et al.,

* Corresponding author.
** Corresponding author.
E-mail addresses: krflore6@asu.edu (K. Flores), jason.parsons@utrgv.edu (J. G. Parsons).

https://doi.org/10.1016/j.jenvman.2024.121160
Received 6 January 2024; Received in revised form 17 April 2024; Accepted 10 May 2024
Available online 17 May 2024
0301-4797/© 2024 Elsevier Ltd. All rights are reserved, including those for text and data mining, AI training, and similar technologies.

2017). Therefore, effective physical-chemical separation of chromium from water sources is urgently needed.

Techniques for removing chromium from polluted waters include chemical precipitation, ion exchange, membrane separation, biosorption, photocatalytic reduction, and adsorption (Babapour et al., 2022; Kenfoud et al., 2022; Nur-E-Alam et al., 2020). Adsorption of heavy metal ions from polluted water has been championed in recent years due to its effectiveness, simplistic operation, minimal energy requirements, and economic feasibility (Chen et al., 2022; F. Liu et al., 2023b). Carbon based adsorbents have been heavily studied over the years due to their high adsorption capacities, substantial degree of functionalization, and regenerative capabilities (Baby et al., 2019; Mariana et al., 2021). Biochars (BC) are sustainable carbon adsorbents produced from biological wastes. These materials have been heavily studied for adsorption processes due to their high surface area, developed pore structure, and robust mechanical properties (Fang et al., 2023; Liang et al., 2021; Lu et al., 2022). Utilizing everyday waste sources for biochar (BC) production can generate highly effective adsorbents at low costs (Liu et al., 2023c). Common agricultural waste products can be easily processed/repurposed as inexpensive active ingredients for water purification technologies (Li et al., 2021). For green adsorption technologies to have an impact on the growing societal demand for clean water, maximized efforts must come from an approach where treatment costs are low and remediation effectivity is high (Gupta et al., 2009). Adsorbent surface modification can be used to enhance adsorption capacity, as well as selectivity, of target pollutants such as heavy metals through incorporation of specific chemical functional groups (Liu et al., 2021b; Qiu et al., 2022). The agricultural sector is one of the highest water consumption industries across the globe (Alcamo et al., 2000). Therefore, a circular economic strategy where crop waste could be repurposed to purify the surrounding polluted water sources would ensure sustainable water consumption and serve as a paradigm for other circular economic strategies.

Herein, we have developed, tested, and optimized an amino modified biochar adsorbent for the targeted removal of both Cr(VI) and Cr(III) from aqueous solutions. The biochar was synthesized through the pyrolysis of an agricultural waste (pineapple skins) to generate a pristine BC adsorbent. The pristine BC was then modified, through a green chemical method, to introduce amino groups onto the surface of the adsorbent and was termed as the amino modified BC. Both adsorbent materials were tested in tandem for Cr(VI) and Cr(III) removal capability, to observe the effect that chemical modification had on the adsorption properties of these materials. The modification was shown to greatly enhance adsorption of both Cr species. The Cr(VI) loading capacity was increased by over 10-fold, and a 6-fold increase was observed for Cr(III), when compared with the pristine BC absorbent. The Cr(VI) and Cr(III) adsorption proceeded through a spontaneous manner for the amino modified variety, while the pristine was found to only be spontaneous for Cr(III) adsorption at 25 °C. Interference studies showed excellent selectivity for Cr(VI) over other common anionic species, even at concentrations 3,000× that of the chromium species.

2. Materials and methods

2.1. Synthesis of pristine biochar

Locally sourced smooth cayenne pineapples were washed using 18 mΩ/cm deionized water, cut, and separated into the fruit and skin portions. The pineapple skins were placed in a Pyrex dish and allowed to dry in an oven at 65 °C, for a period of one week, until all the biomass was completely dry. After drying, the pineapple skins were blended in an industrial grade food processor. The resulting powder was then passed through a 125 μm sieve, to remove any larger sized particles. The sieved powder was then placed in a ceramic crucible and heated in a tube furnace, with Ar gas flowing, to a temperature of 350 °C for a period of 1 h. Following the pyrolysis, the resulting powder was allowed to cool to room temperature, then ground once again with a mortar and pestle. The mass of produced pristine BC was then taken to calculate the product yield.

2.2. Amino modification of biochar

The amino modification of the biochar materials proceeded through a facile chemical synthesis process (G.-X. Yang and Jiang, 2014). In brief, 100 mL of 1:1 mixture of HNO_3/H_2SO_4 was placed in a 250 mL round-bottom flask and allowed to cool in an ice bath (4 °C). A total of 6.0 g of the pristine biochar material was added to the acid mixture and was stirred magnetically for 2 h. The acidic mixture causes a nitration reaction to occur, resulting in introduction of $–NO_2$ groups onto the structure of the BC adsorbent. Following the nitration reaction, the resulting product was allowed to cool, then filtered using a fritted glass filter and washed with several portions of isopropanol. The powder was then dried overnight at a temperature of 50 °C to remove any residual moisture. After drying, the BC was added to a three-neck round bottom flask followed by 50 mL of ultra-pure H_2O and 20 mL of 15 M NH_4OH. The reaction was stirred for 15 min, followed by the addition of 28 g of Na_2SO_4, and then allowed to continue stirring for a period of 24 h. After this time, 120 mL of 2.9 M acetic acid was added to the flask, and the solution was then refluxed at a temperature of 100 °C for 5 h. The acetic acid acted as a proton (H^+) source to ensure the complete reduction and conversion of the NO_2 to NH_2 groups. The resulting product was cooled, the amino modified BC was collected through vacuum filtration, and finally dried overnight at 50 °C.

2.3. Analytical instrumentation

Fourier-transform infrared spectroscopy (FTIR) data was collected on a Perking Elmer Frontier model equipped with a universal total attenuated reflection attachment. The FTIR analysis was conducted from 600 to 4000 cm^{-1} with a resolution of 4.0 cm^{-1}. A Zeiss LS10 EVO scanning electron microscope (SEM) microscope was utilized for imaging of the adsorbent materials. The SEM images were collected at a working voltage of 20 kV and an operating current of 2.5 A. The working distances of the SEM ranged from 6.0 mm to 4.5 mm for the low and high magnification micrographs respectively. The SEM was equipped with an energy dispersive spectroscopy (EDS) unit. The EDS data was collected at a working voltage of 50 kV at an optimum working distance of 8.0 mm. Samples were sputter coated using an Au–Pd target to enhance sample conductivity and in turn improve image quality. X-ray diffraction was collected using a Bruker D2 X-ray diffractometer equipped with a cobalt source (K_α = 1.789 Å), an iron filter, operated at 300 W of power, and a scintillation detector. The data were collected from 10 to 75° in 2θ with a 5s counting time, and a step of 0.05°. The surface area and porosity data were collected using a Quantachrome Nova 2200e. The Brunauer-Emmett-Teller (BET) surface area and Pore Volume were determined using N_2 adsorption isotherm at 77 K.

Concentrations of chromium species were quantified using inductively coupled plasma optical emission spectroscopy (ICP-OES) analysis for metal quantification. A PerkinElmer Optima 8300 DV ICP-OES instrument was utilized for Cr concentration determination. Typical operating parameters include a plasma flow rate of 15 L/min, a nebulizer flow of 0.55 L/min, and a sample flow rate of 1.5 mL/min. Each analysis was the average of three replicates with an integration time of 20 s. A Cyclonic spray chamber, a GemCon nebulizer, and a 2.0 mm alumina injector were equipped on the instrumental configuration, which was operated at an RF power of 1500 W and λ = 276.2 nm.

2.4. Adsorption test procedures

Effects of initial pH conditions were analyzed for the binding of Cr (VI) and Cr(III) upon the pristine and amino modified BC, from a pH range of 2–5. Solutions containing either 300 μg/L of Cr(VI) or Cr(III)

were pH adjusted using dilute nitric acid or sodium hydroxide. A total mass of 10 mg of the adsorbent material was added to 5 mL test tube, then combined with 4 mL of the pH adjusted chromium solution. The resulting mixtures were then capped and placed on a bench top nutating mixer and allowed to equilibrate for 1 h. Following equilibrium, samples were centrifuged for a period of 5 min at a speed of 3600 rpm. The supernatants were decanted and transferred to a separate tube and saved for ICP-OES analysis. Control samples, containing no adsorbent, were also performed in tandem for all adsorption studies. All experiments were performed in triplicate to ensure reproducibility.

Adsorption studies were performed at different time intervals to compare the difference in binding capacity (mg/g) between the two adsorbents over a reaction period of 2 h. Time dependency studies were performed with 30 ppm Cr(VI) or Cr(III) solutions adjusted to optimum pH conditions, as determined from the previous pH study. A total mass of 10 mg of adsorbent was added to 5 mL test tubes, followed by 4 mL of the Cr containing pH adjusted solutions, the tubes were then equilibrated on nutating mixer for various times. The time frames were: 5, 10, 15, 30, 60, 90, and 120 min of interaction of the absorbent with the Cr containing solutions. After the various time points, samples were centrifuged, separated, and analyzed.

Isotherm experiments were performed to study the thermodynamic properties of the adsorption of Cr(VI) and Cr(III) to both the pristine and amino modified BC adsorbents. These studies were performed over the period of 1 h under optimum pH conditions. A range of various Cr concentrations were utilized for isothermal adsorption studies including 0.3, 3.0, 30, 90, 300, 1000 ppm of either Cr(VI) or Cr(III). Reactions were performed at three different temperatures (4, 25, and 45 °C) to measure the temperature dependance of the adsorption processes. After the studies were completed, the samples were centrifuged, decanted, and analyzed using ICP-OES for chromium quantification.

The effects of coexisting ions were tested for both Cr(VI) and Cr(III) binding to the amino modified and pristine BC adsorbents. 0.3 ppm of Cr (VI) solutions were spiked with 0.3, 3, 30, 300, and 1000 ppm of Cl^-, NO_3^-, SO_4^{2-}, PO_4^{3-}, SiO_3^{2-}, and CO_3^{2-}. Solutions of 0.3 ppm of Cr(III) were spiked with Na^+, K^+, Ca^{2+}, and Mg^{2+} cations at concentrations of 0.3, 3, 30, 300, and 1000 ppm. These solutions were pH adjusted to the optimum binding pH for adsorption testing following prior procedures. Once adsorption interference studies were completed, samples were centrifuged, decanted, and analyzed via ICP-OES.

3. Results and discussion

3.1. Characterization of pristine and amino modified biochar adsorbents

The pineapple skin sourced biochar was characterized using FTIR-ATR analysis, before and after the amino modification, to assess the effective functionalization of the adsorbent material. As can be seen in Fig. 1, both the pristine and amino modified adsorbents displayed a variety of absorption peaks across their spectra. Beginning with the pristine biochar C–H bending (750 & 870 cm^{-1}), C–O stretching (1105 cm^{-1}), S=O stretching (1370 cm^{-1}), O–H bending (1430 cm^{-1}), C=C/N–O stretching (1575 cm^{-1}), C–H bending (1980 cm^{-1}), S–C ˆ N stretching (2165 cm^{-1}), and finally C–H stretching (2920 cm^{-1}) were observed (Infrared Spectroscopy Absorption Table, 2020; IR Spectrum Table and Chart, 2023). In the amino modified BC, it should be noted the absence of the first two C–H bending peaks, when compared to the pristine BC, and emergence of a new C–N stretching peak (1030 cm^{-1}) (Kumar et al., 2017). Peaks for C–O stretching (1105 cm^{-1}) and S]O stretching (1370 cm^{-1}) seemed to be maintained from the pristine BC structure. The C]C/N–H peak (1590 cm^{-1}) peak identified in the amino modified BC seems to have shifted from the original 1575 cm^{-1} position in the pristine BC, identifying a shift in nitrogen binding from N–O in the pristine to N–H in the amino modified biochar (H. Liu et al., 2019; Ryu et al., 2010). The C–H bending (1980 cm^{-1}) and S–C ˆ N stretching (2165 cm^{-1}) were also maintained from the pristine BC structure, just at lower absorption intensities. From the comparison of the structures, the introduction of new C–N and N–H bonds are observed in the modified BC along with a depletion of N–O and C–H bonds. These results allow for the inferring of successful amino modification of the biochar adsorbent.

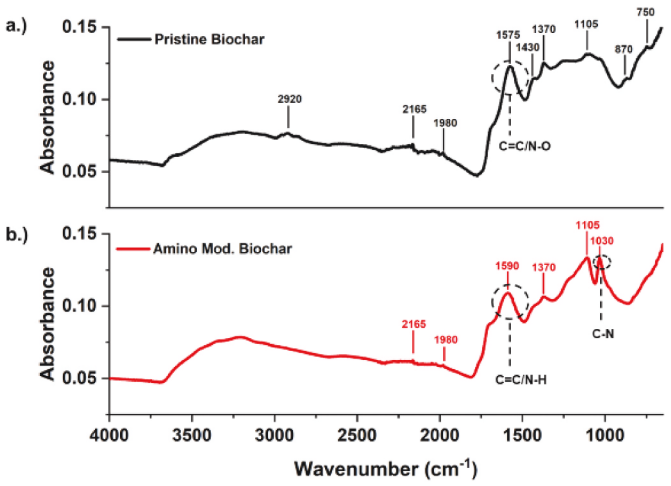

Fig. 1. FTIR-ATR characterization of (a) pristine and (b) amino-modified biochar.

Adsorbent surface imaging by SEM was performed on both the pristine and amino modified BC to investigate the morphology and structure of these materials before and after the chemical modification. The SEM image of the pristine BC can be found in Fig. 2a, while the amino modified version can be seen in Fig. 2b. The SEM analysis of the pristine BC revealed an amorphous structure with micron sized plates dispersed across the surface. Similar appearance and structure has been reported in studies utilizing BC and other graphitic materials (Q. Li et al., 2018; Quan et al., 2018; C. Wang et al., 2016). There appears to be a high amount of surface roughness with many craters and grooves across the pristine biochar surface. In comparison, the amino modified variety displays a smoother surface with areas of aggregated platelets.

Fig. 3 shows the collected XRD patterns for the pristine and amino modified biochar as synthesized. As can be seen in the diffraction patterns both samples are amorphous and show diffraction patterns similar to other biochar and carbon black samples(W. Chen et al., 2016; Keiluweit et al., 2010; Y. Liu et al., 2012; Park et al., 2010; Yoo et al., 2018). The XRD of the pristine BC shows a broad weak peak around 20–32 in 2θ, which correlates to 18–27 in 2θ for a Cu source and is in the same diffraction range as sample shown in the literature. The broad weak peak is generally labelled the (002) diffraction plane and is commonly observed in non-graphitizing carbon samples (Keiluweit et al., 2010; Park et al., 2010; Yoo et al., 2018). The weak diffraction peak is considered to be a remnant of the cellulose structure, similar to other BCs synthesized at low temperatures (Keiluweit et al., 2010; Park et al., 2010; Yoo et al., 2018). The weak diffraction peak in the amino modified biochar appears to be slightly shifted to a higher diffraction angle compared to the pristine biochar. The shift in the position of the diffraction peak may be due to the treatment of the sample during the modification process where remnant material was washed out of the sample.

3.2. Optimum pH for Cr(VI) and Cr(III) adsorption

The optimum pH conditions for chromium species adsorption to both pristine and amino modified BC were determined using 300 ppb solutions of either Cr(VI) or Cr(III) under different pH conditions. Pristine BC showcased an optimum pH for Cr(VI) removal at pH 2.0, with approximately 40% removal observed after 1 h of treatment, as shown in Fig. 4. However, the amount of Cr(VI) adsorbed decreased to less than 10% binding at higher pH conditions. This trend can be explained by the

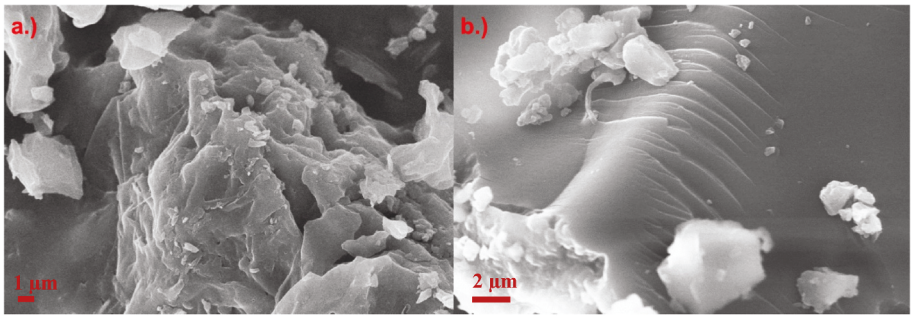

Fig. 2. Micrographs obtained by scanning electron microscopy (SEM) of (a) pristine and (b) amino modified biochar.

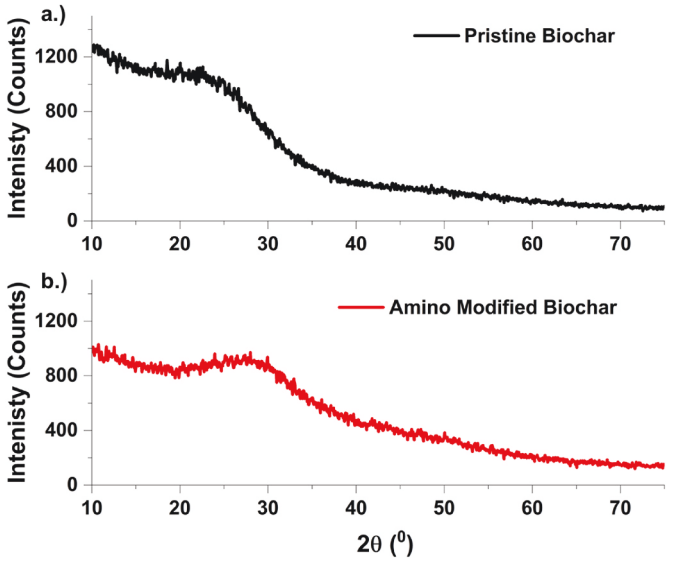

Fig. 3. X-ray powder diffraction of the pristine biochar(a) as well as the amino modified variety (b).

overall surface charge of BC in function of pH. Organic functional groups of BC are generally positively charged at pHs below ~3.0. Positively charged adsorbent benefits electrostatic attraction of negatively charged anionic species of chromium (VI) (e.g., CrO_4^{2-}, $HCrO_4^-$, $Cr_2O_7^{2-}$) (Selomulya et al., 1999). While at the lower pHs, it is well known that the $HCrO_4^-$ form is the preferential speciation of Cr(VI) according to its characteristic pK_a values following acid-base reaction equilibria of equations (1) and (2). The pH dependent speciation of Cr(VI) can be found in Fig. 4c below, with respect to the aforementioned pK_a values. Above pH ~3.0 the BC become negatively charged which was detrimental for the adsorption of negatively charged species of Cr(VI) given the increasing electrostatic repulsion (specially for divalent anionic species).

$$H_2CrO_4^- \leftrightharpoons H^+ + HCrO_4^- \quad pK_{a1} = -0.8\text{–}1.6 \qquad \text{(Eq 1.)}$$

$$HCrO_4^- \leftrightharpoons H^+ + CrO_4^{2-} \quad pK_{a2} = 6.51 \qquad \text{(Eq 2.)}$$

Similar binding trends for Cr(VI) have been observed for other nano-adsorbents, biochar, and activated carbon particles (Cantu et al., 2014; Parsons et al., 2002; Selomulya et al., 1999). This could stem from the similar point of zero net charge (PZNC) for pristine BC, like many other carbonaceous adsorbents, occurring between pH 2.0 and 2.6 (Dehouli et al., 2010; Kosmulski, 2011; Silber et al., 2010). The adsorbent surface remains negatively charged beyond this characteristic PZNC value. Conversely, this surface charge transition in function of pH is beneficial for the removal of positively charged chromium (III) cationic species (i.e., Cr^{3+}, $Cr(OH)^{2+}$, $Cr(OH)_2^+$)) as deduced from Fig. 4a.

For the amino modified BC an appreciable increase in Cr(VI) binding (≈80%) was observed at all pHs. A maximum binding was observed at pH 3.0 with 95% removal, while pH 4.0 and 5.0 maintained excellent binding with over 90% removal. To have a direct comparison of the pristine BC and the amino modified BC, a pH of 2.0 was set for all future Cr(VI) adsorption studies. The difference in binding trends between the pristine and amino modified BCs indicates different attractive forces participating in their adsorption, with a more effective mechanism identified in the amino variety. The amino biochar clearly attained a higher degree of adsorption, at more environmentally relevant pH conditions. The functionalization of amino groups on the modified biochar induces a greater positive surface charge via N–H groups in the modified, vs N–O groups present in the pristine variety, generating greater propensity for electrostatic interaction between the amino BC and the Cr(VI) anion(F. Liu et al., 2021a). In addition, possible hydrogen bonding and complexation could synergize the Cr(VI) adsorption mechanism further, which has been a reported adsorption mechanism for other amino modified adsorbents (S. Chen et al., 2011; Miretzky and Cirelli, 2010; Nkuigue Fotsing et al., 2021).

In both BCs pH 4.0 was considered optimal for Cr(III) binding with nearly 75% removal for the pristine and over 95% for the amino-modified BC. This general trend has been well observed for Cr(III) binding with different adsorbents (Miretzky and Cirelli, 2010). The decreased binding at lower pH levels is believed to occur due to greater levels of protonation occurring on the biochar materials. In highly acidic conditions (pH ≤ 2) the positive surface charge of these materials would repel Cr(III) cations in solution. The improved Cr(III) adsorption with the amino modified BC, at all pHs, indicates additional interactions, aside from just electrostatic, could be contributing to the adsorption mechanism. As can be seen in Fig. 4d, the speciation of Cr(III) in terms of pH, exists in the different species throughout the 2–5 pH range. As the reaction solution becomes less acidic the $Cr(OH)^{2+}$ and $Cr(OH)_2^+$ species become more prevalent resulting in additional possible adsorption interactions. Complexation of Cr(III) via amine groups has been reported for *Chlorella miniate* biosorbent, as well as for aminated polyacrylonitrile (APANFs) adsorbent (S. Deng and Bai, 2004; X. Han et al., 2006). In the later, it was reported that complexation of Cr(III) with the nitrogen groups of the APANFs was the observed adsorption mechanism, which could be contributing to the improved Cr(III) adsorption in the amino modified BC. Thus, similar amino-complexation is expected to be enabled in the amino-modified BC.

3.3. SEM-EDS analysis of BC following chromium binding

The SEM-EDS analysis was performed on both BC materials to elucidate changes to surface elemental distribution after amino modification, and the effect that might have on Cr(VI) and Cr(III) binding. Fig. 5 displays electron maps generated from this analysis where sulfur, oxygen, nitrogen, carbon, and chromium were mapped on the surface of both pristine and amino modified biochar after equilibration with 100 ppm of Cr(VI) at pH 2, and 100 ppm of Cr(III) at pH 4. Note that the

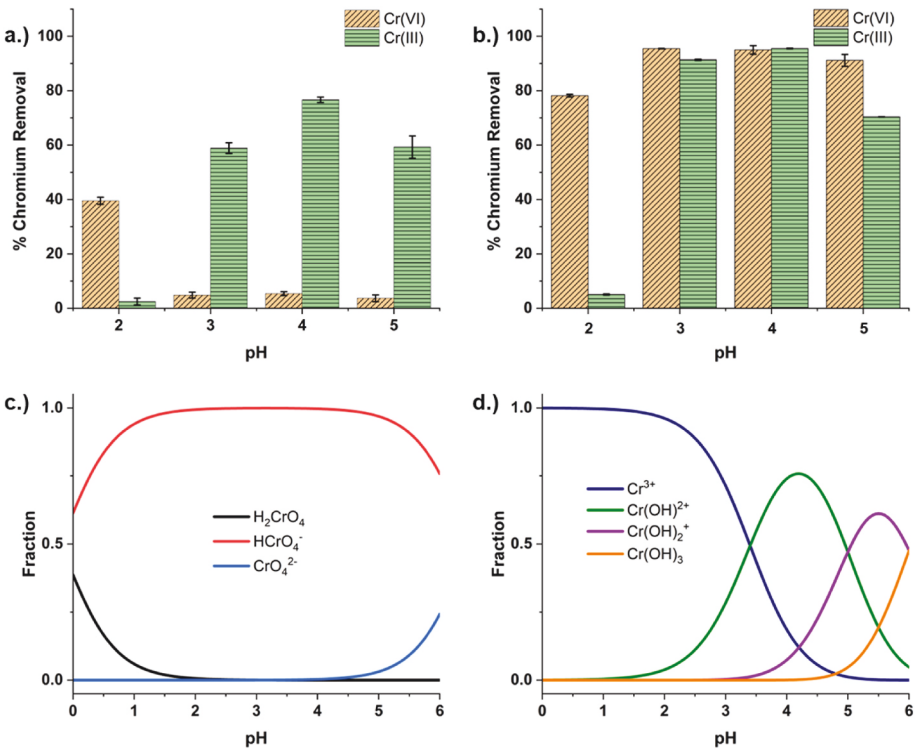

Fig. 4. % Chromium Removal for the pristine biochar (a) the amino modified biochar (b) pH dependent speciation of Cr(VI) (c) and pH dependent speciation of Cr (III) (d).

presence of these elements agrees with the FTIR-ATR spectra of Fig. 2, that identified S]O, C–O, and N–O stretching among other relevant signals. As can be seen in Fig. 5 a & b there is a difference between the adsorption pattern of Cr(VI) binding to the pristine and amino modified BCs. Adsorbed Cr on pristine BC appears to be randomly distributed; whereas amino-modified BC shows more densely concentrated areas of Cr adsorption following a similar pattern to the areas mapped for nitrogen. Thus, it can be inferred that a correlation between Cr and the amino functional groups, for the amino-modified BC, exists. This trend supports the hypothesis of the discussed adsorption mechanism enhancement by hydrogen bonding and or complexation of chromium, as has been reported in other accounts of heavy metal adsorption(Jin et al., 2022). In Fig. 5 c and d, Cr(III) adsorption for both the native and amino modified BCs show a similar homogenous distribution. In both the Cr(VI) and Cr(III) adsorption the amino modified BC displayed brighter Cr mapping, indicating higher adsorption for the chemically modified BC.

3.4. Time dependency studies and kinetic modeling

Time dependent studies for the adsorption of chromium ions to both amino modified and pristine BC were performed to measure the loading capacity (Qt (mg/g)) for both Cr(VI) and Cr(III) over 120 min of reaction time. Adsorption studies were fitted to a Langmuir adsorption model. The results of time dependency studies are shown below in Fig. 6 for both the amino modified and pristine BC adsorbents.

Adsorption capacities for both Cr(VI) and Cr(III) were much higher in the amino modified BC, over the entire extent of the reaction. As can be seen in the plot from Fig. 6, the loading equilibrium is reached rapidly with the amino variety. Maximum loading capacities were observed within a 1-h period and remained relatively constant thereafter. Furthermore, 67% of Cr(VI) & 81% Cr(III) of adsorption was accomplished in the first 5 min of contact for the amino BC, while 43% of Cr (VI) and 44% of Cr(III) were observed for the pristine BC. To compare the performance of the two adsorbents, the instantaneous rate of adsorption was calculated at the 5-min mark of the reaction. Adsorption rates are summarized in Fig. 6. The reaction rates observed for the amino BC were much higher than those observed for the pristine BC, showing an improvement of 18-fold for Cr(VI) and 32-fold for Cr(III). For both chromium ions the amino modified BC surpassed a 20 mg/g loading within 15 min of contact with Cr solution, highlighting rapid adsorption compared to similar adsorbents (Babu and Gupta, 2008; "Efficient Removal of Cr(VI) from Aqueous Solution onto Palm Trunk Charcoal," 2016; Ksakas et al., 2015; Partlan et al., 2020). The speed of the adsorption process would have major impact on the treatment capability, volume of polluted water which can be effectively remediated, which in turn directly affects the scalability of such technologies (Hui et al., 2018; J. Wang and Guo, 2020; Zhou et al., 2020).

Results of the kinetic studies are shown in Fig. 7 for both the unmodified and modified biochars and was found to follow an intraparticle kinetics model. The equation is given below (Ho and McKay, 1998):

$$Q_t = kt^{0.5} \quad \text{(Eq 3.)}$$

where Q_t is the mass of metal adsorbed by the adsorbent at a specific time, k is the rate constant, and $t^{0.5}$ is the square root of the reaction time. This kinetics model has been used to effectively describe the binding of different metal ions and organic molecules to biochars (Blanchard et al., 1984; Ho and McKay, 1998; Weber and Morris, 1963). In addition, kinetics indicate there are possibly two sites on the biochar for Cr binding, one that is easily available and a secondary adsorption site that is not readily accessible by the metal ions. In the present work kinetics showed a reliance on temperature, similar to the thermodynamics studies in the following section. The rate of the Cr(III) binding to the pristine biochar proceeded as an endothermic reaction, whereas the Cr(VI) binding to the pristine biochar followed an exothermic reaction. The kinetics of both the Cr(III) and Cr(VI) binding to the amino biochar followed an exothermic where the rate of binding decreased with increasing temperature, which is further confirmed in thermodynamics studies. Kinetics were studied utilizing a split kinetics model, where the

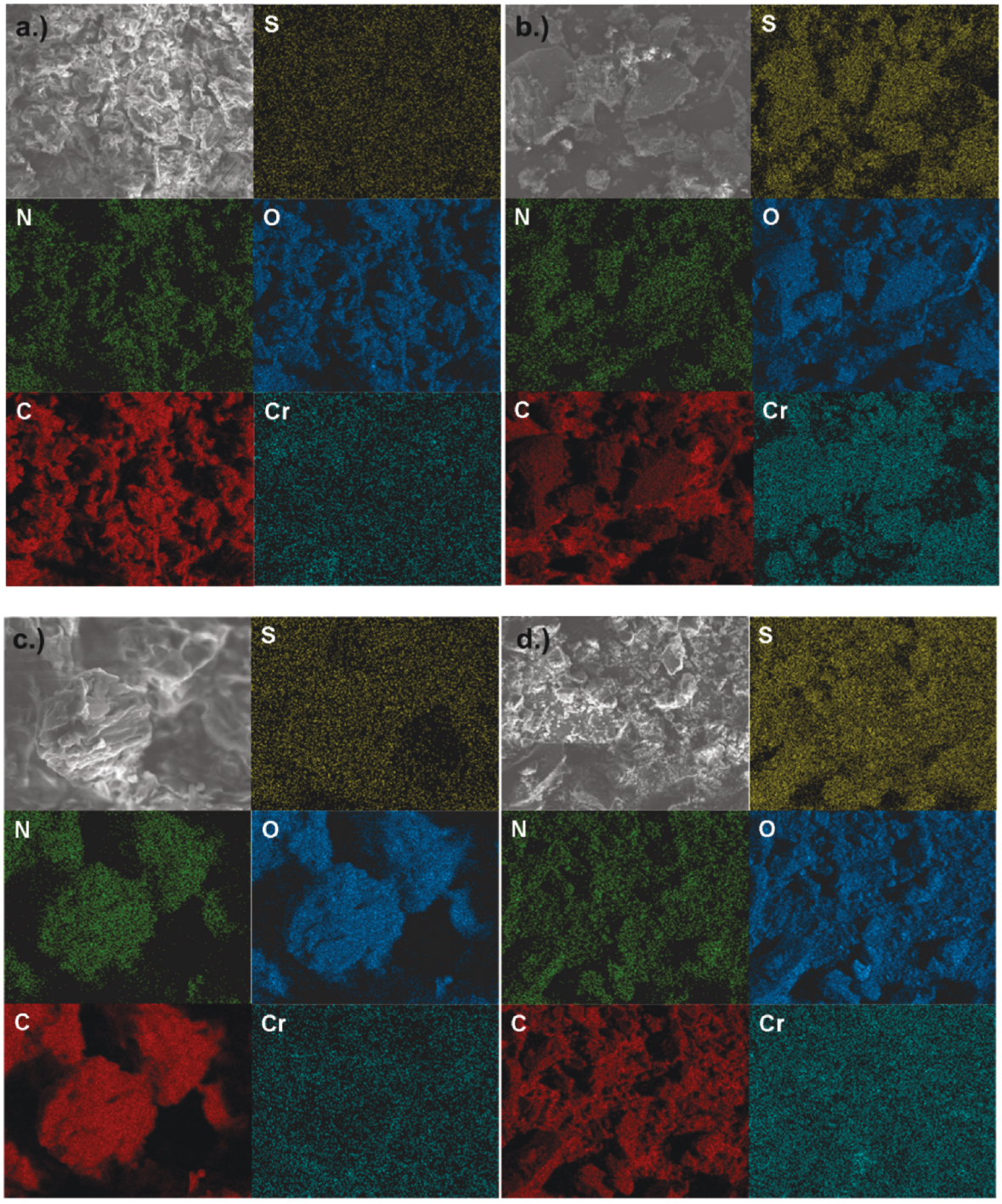

Fig. 5. Pristine Biochar equilibrated with Cr(VI) at pH 2 (a) Amino modified Biochar equilibrated with Cr(VI) at pH 2 (b) Pristine Biochar equilibrated with Cr(III) at pH 4 (c) Amino modified Biochar equilibrated with Cr(III) at pH 4(d).

reaction was broken down into two separate portions utilizing first order kinetics. The data from the split first order kinetics model indicates two different processes were occurring for Cr(III) and Cr(VI) binding to both biochar materials (Summarized in Table 1). The first reaction consistently had a higher rate constants than the second reaction, giving further indication of the mechanism occurring in 2 steps with the exception of Cr(III) adsorption by the pristine at 4 °C. However, this is not a second order rection but rather a two-step process, which may be occurring due to site accessibility. As noted in the time dependency studies, the majority of the binding occurs within the first 5 min of contact, then slows and becomes relatively stable over the remainder of the contact time. However, the fittings of the kinetics using the intraparticle diffusion model overall have higher correlation coefficients and are more representative of the binding process as shown in Table 1. The fitting results for the zeroth order, first order and second order kinetics are shown in Table 2. As can be seen in Table 2, the majority of the fittings for traditional kinetics are unacceptable with correlation coefficients for the most part below, below 0.95. Intraparticle diffusion model can be pore related or surface diffusion related, due to the carbonized structure of cellulose structure after biochar synthesis the surface could be diffusion limited (J. Wu et al., 2022) The rates of the reaction are significantly enhanced after the amino modification of the

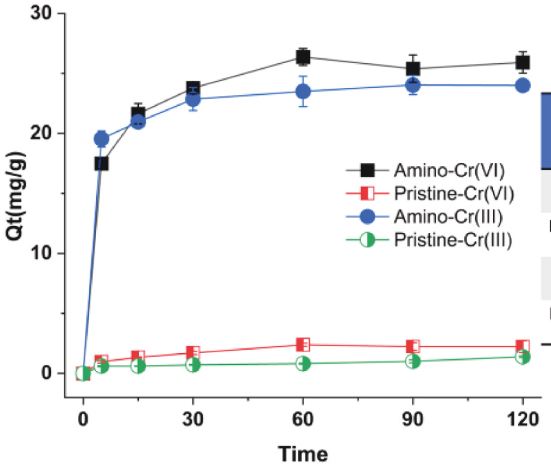

Adsorbent	Instantaneous Rate of Adsorption (mg/g·min)
Amino BC – Cr(VI)	3.496
Pristine BC – Cr(VI)	0.194
Amino BC – Cr(III)	3.908
Pristine BC – Cr(III)	0.121

Fig. 6. The adsorption capacity of Amino and Pristine BC for both Cr(VI) and Cr(III) as a function of time (plot) and the instantaneous rate of adsorption at 5 min expressed as mg of metal per gram of adsorbent per minute. Reaction performed at 22 °C.

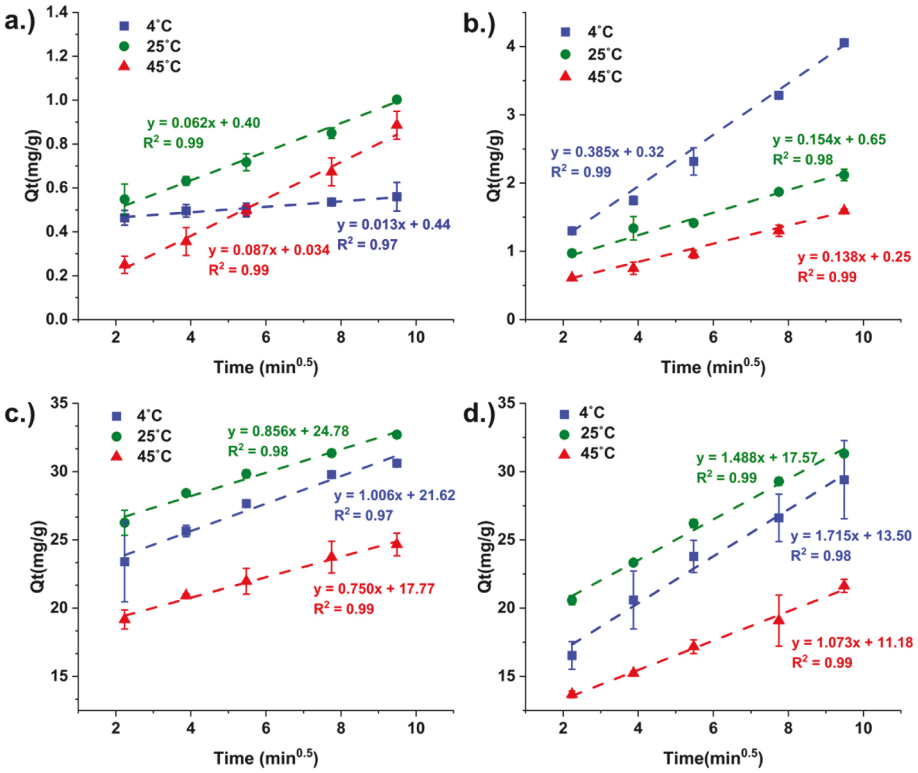

Fig. 7. Intraparticle kinetics for pristine BC adsorption of Cr(III) and Cr(VI) (a & b) as well as the amino modified BC (c &d).

biochar, for both Cr(III) and Cr(VI) adsorption to the amino modified BC. Similar trends in kinetics enhancement have been observed in the literature after chemical modification(Ekanayake et al., 2022; Kołodyńska et al., 2012).

3.5. Thermodynamics for chromium adsorption

The thermodynamics of the chromium adsorption process was analyzed to establish trends in temperature dependence and to further investigate the energetics of adsorption mechanism for both adsorbents. The first step in these calculations came in relating the equilibrium constant (K_d) to the Gibbs free energy as shown in equation (3) below (Saha and Chowdhury, 2011).

$$\Delta G^{\circ} = -RT\,ln(K_d) \quad \text{(Eq 3.)}$$

The K_d is then related to the enthalpy (ΔH°) and entropy (ΔS°) of the adsorption mechanism as based in the relationship between equations (4) and (5).

$$\Delta G^{\circ} = \Delta H^{\circ} - T\Delta S^{\circ} \quad \text{(Eq 4.)}$$

$$\ln(K_d) = \frac{\Delta S^{\circ}}{R} - \frac{\Delta H^{\circ}}{RT} \quad \text{(Eq 5.)}$$

By plotting the natural log of the equilibrium constant against the inverse of temperature in Kelvin (1/T) a linear plot was generated with the slope representing -ΔH°/R of the adsorption reaction. The entropy of the same adsorption reaction is the determined from the intercept (ΔS°/

Table 1
Summary of the kinetics data fittings using a two process zero order kinetics model and the intraparticle diffusion model.

Sample	K_1 (mg/g/min)	R_1^2	$K_{1\text{-}2}$ (mg/g/min)	$R_{1\text{-}2}^2$	K_{ip} (mg/g/min$^{0.5}$)	R^2
Cr(III) Pristine Biochar 4 °C	0.0026	0.97	0.0050	0.90	0.0130	0.97
Cr(III) Pristine Biochar 22 °C	0.0067	0.99	0.0048	1.0	0.0620	0.99
Cr(III) Pristine Biochar 45 °C	0.0099	0.99	0.0065	1.0	0.0870	0.99
Cr(VI) Pristine Biochar 4 °C	0.0405	1.0	0.0290	1.0	0.3850	0.99
Cr(VI) Pristine Biochar 22 °C	0.0167	1.0	0.0120	0.97	0.1540	0.98
Cr(VI) Pristine Biochar 45 °C	0.0140	1.0	0.0110	1.0	0.1380	0.99
Cr(III) Amino Modified Biochar 4 °C	0.1680	0.98	0.0490	0.94	1.006	0.97
Cr(III) Amino modified Biochar 22 °C	0.1400	0.95	0.0480	0.99	0.856	0.98
Cr(III) Amino modified Biochar 45 °C	0.1090	0.93	0.0450	0.97	0.750	0.99
Cr(VI) Amino modified Biochar 4 °C	0.2870	0.97	0.0940	1.00	1.715	0.98
Cr(VI) Amino modified Biochar 22 °C	0.2220	0.99	0.0850	0.99	1.488	0.99
Cr(VI) Amino modified Biochar 45 °C	0.1380	0.99	0.0740	0.99	1.073	0.99

Table 2
Summary of Kinetics fittings for zero order, first order, and second reactions for the entire data set.

Sample	K_0 (mg/g/min)	R_0^2	K_1	R_1^2	K_2	R_2^2
Cr(III) Pristine Biochar 4 °C	0.0053	0.99	0.0020	0.94	0.0040	0.93
Cr(III) Pristine Biochar 22 °C	0.0072	0.99	0.0067	0.97	0.0091	0.94
Cr(III) Pristine Biochar 45 °C	0.0100	0.95	0.0139	0.92	0.0297	0.81
Cr(VI) Pristine Biochar 4 °C	0.0322	0.95	0.0083	0.9	0.0057	0.82
Cr(VI) Pristine Biochar 22 °C	0.0127	0.95	0.0128	0.94	0.0056	0.85
Cr(VI) Pristine Biochar 45 °C	0.0115	0.99	0.0110	0.96	0.0112	0.9
Cr(III) Amino Modified Biochar 4 °C	0.0804	0.89	0.0030	0.87	0.00011	0.84
Cr(III) Amino modified Biochar 22 °C	0.0690	0.91	0.0023	0.89	0.00008	0.87
Cr(III) Amino modified Biochar 45 °C	0.0607	0.93	0.0027	0.91	0.00013	0.89
Cr(VI) Amino modified Biochar 4 °C	0.1383	0.91	0.0060	0.86	0.0003	0.80
Cr(VI) Amino modified Biochar 22 °C	0.1208	0.94	0.0046	0.91	0.0002	0.87
Cr(VI) Amino modified Biochar 45 °C	0.089	0.98	0.0051	0.96	0.0003	0.93

R) of the line multiplied by the gas constant (R).

Thermodynamic data was generated through adsorption isotherms performed at three temperatures 4, 25, and 45 °C. The results of these isotherm studies were found to best fit a Langmuir isotherm model, which indicates a monolayer adsorption for both Cr ions, aside from the small degree of pore diffusion discussed in the previous section (Togue Kamga, 2019; Zaheer et al., 2019). Fig. 8 displays the adsorption thermodynamic plots for both Cr(VI) and Cr(III) binding to the pristine BC adsorbent. For the pristine BC Cr(VI) adsorption proceeded through an exothermic process, as can be seen in Fig. 8. The negative value for the ΔH of the reaction further supports an exothermic nature for Cr(VI) adsorption on the pristine BC. Alternatively, Cr(III) adsorption was found to proceed through an endothermic nature for pristine BC. The positive ΔH for the reaction supports an endothermic process for Cr(III) adsorption, while similar thermodynamic trends have been observed for Cr(III) adsorption upon graphitic adsorbents (Bai et al., 2020; S. Yang et al., 2014). For the amino modified BC, Cr(VI) adsorption proceeded through an exothermic process. The exothermic nature is validated by the – ΔH calculated for this reaction and has been observed for other bioderived and graphitic adsorbents utilized for Cr(VI) adsorption (Akram et al., 2017; Cho et al., 2011; Miretzky and Cirelli, 2010). Adsorption of Cr(III) upon the amino modified adsorbent revealed an opposite thermodynamic trend to that of the pristine BC, with an exothermic trend observed (ΔH = −40.96 kJ/mol). The difference in temperature dependency between the adsorbents, as well as differences in spontaneity arising from the amino modification, exemplifies clear differences in the adsorption mechanism occurring on these materials.

From the thermodynamic data presented, the amino modified BC displayed spontaneous adsorption to both Cr(VI) and Cr(III) at room temperature, while the pristine BC was only spontaneous to Cr(III). This data indicates that the amino modification shifted N–O moieties in the pristine biochar to N–H moieties, decreasing the negative surface charge allowing for greater interaction with negatively charged Cr(VI) sources. As discussed in section 3.2, the possibility of hydrogen bonding and complexation, could be further facilitating this spontaneous adsorption of Cr(VI). While the thermodynamic calculations are helpful in finding temperature dependence and probing the energetics of the process, all values reported from these calculations are small in magnitude (near equilibrium) and are indicative of a physical adsorption process (Auta and Hameed, 2012; Q. Li et al., 2010).

The binding capacities for these adsorbent materials can be found in Fig. 9 showing greatly improved binding capacity for amino modified adsorbent, most notably for the Cr(VI) pollutant. With a binding capacity of 46.5 mg/g of Cr(VI) in the amino modified BC compared to 4.11 mg/g for the pristine BC, a 10× improvement in binding capacity was observed in the modified adsorbent. With regards to Cr(III) removal, the modified variety expressed a capacity of 27.1 mg/g, while the pristine BC was determined to be 4.49 mg/g, displaying an approximate six fold improvement in Cr(III) binding. In both instances, a dramatic improvement in the adsorption capacities were observed following the amino modification. Results from BET analysis showed an average surface area of 4.10 m^2/g and 3.02 m^2/g, for the pristine and amino modified BCs, respectively. From this data, we conclude that increased Cr adsorption capacities in the amino modified BC resulted from greater attractive forces between the amino functional groups and the Cr ions, rather than just elevated surface area in the modified adsorbent. These values of surface area are comparable to other low temperature derived BCs, which range from 1.8 to 11.32 (Brewer et al., 2014; W. Chen et al., 2016; Elnour et al., 2019; Guo et al., 2020). The surface area of the biochar was slightly reduced after the amino modification, which may have resulted from the dissolution of graphitic material or nanostructures during the chemical treatment and or filtrations. The removal of such components would result in a diminished surface area per gram for the amino-modified biochar. The chemistry of the biochar synthesized at lower temperatures is different than that of BCs synthesized at higher temperatures and generally have less graphitic structure and

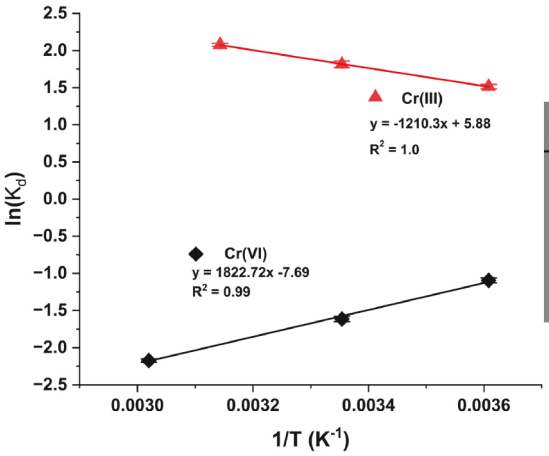

Sample	Temp (°C)	ΔG (kJ/mol)	ΔH (kJ/mol)	ΔS (J/mol)
Cr(VI) Pristine Biochar	4	2.57	-15.15	-63.95
	25	3.91		
	58	6.02		
Cr(III) Pristine Biochar	4	-3.49	10.05	48.84
	25	-4.50		
	45	-5.49		

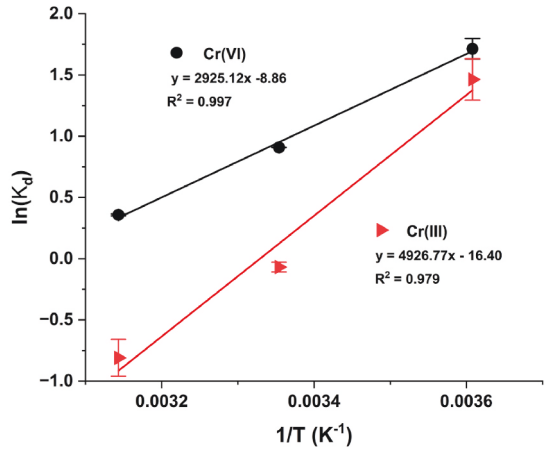

Sample	Temp (°C)	ΔG (kJ/mol)	ΔH (kJ/mol)	ΔS (J/mol)
Cr(VI) Amino Biochar	4	-3.90	-24.32	-73.66
	25	-2.35		
	45	-0.89		
Cr(III) Amino Biochar	4	-3.17	-40.96	-136.36
	25	-0.31		
	45	2.42		

Fig. 8. Results for Isothermal Studies for the adsorption of Cr(VI) & Cr(III) to the pristine biochar (a.), and the amino modified biochar (b.) with the corresponding calculated thermodynmic parameters (ΔG, ΔH, and ΔS) within the tables to the right of the plots.

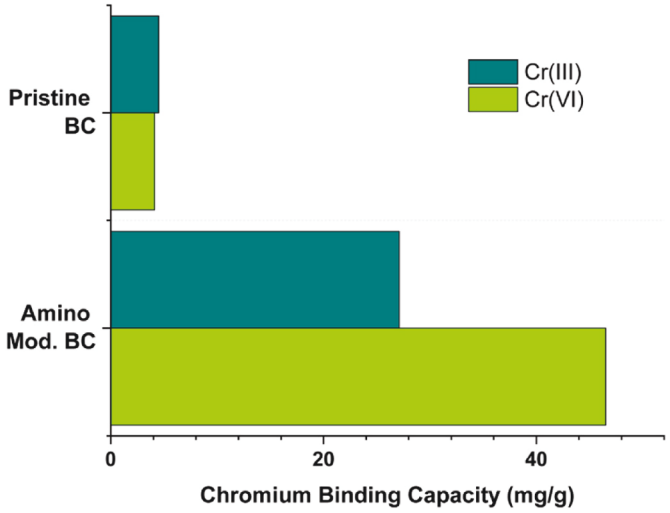

Fig. 9. Binding capacities at 25 °C for Cr(VI) and Cr(III) to both Amino Modified and Prisitne Biochar Adsorbents.

lower surface areas(Brewer et al., 2014; W. Chen et al., 2016; Elnour et al., 2019; Guo et al., 2020).

The amino modified BC achieved competitive binding capacities for both Cr(VI) and Cr(III) species, as can be seen in Table 3 below. This table compares the results from this study to other carbonaceous adsorbents within the literature in terms of binding capacities, as well as the thermodynamics of the binding process. As can be seen in this comparison it is quite rare for materials to have such high adsorption capacities for both species, as the Cr(VI) exists as an anion and Cr(III) as a cation. Such performance highlights the versatility of the amino modified BC for total chromium remediation.

3.6. Interference studies

All previous adsorption studies were conducted in Milli-Q water in order to establish a baseline for the chromium adsorption process. Ground waters, sourced for drinking water, are typically more complex, with varying degrees of ions that could possibly interfer with both Cr(III) and Cr(VI) adsorption. Considering the Cr(VI) sources in these studies expressed a net negative charge, various common anions were tested to observe their effect on Cr(VI) removal. These common anions include Cl^-, NO_3^-, SO_4^{2-}, PO_4^{3-}, SiO_4^{2-}, & CO_3^{2-} (Hautman et al., 1999; Le et al., 2011; Zheng et al., 2021). For the pristine BC, a 40% chromium removal was observed for Cr(VI) in the simplistic Milli-Q (18 MΩ/cm) water matrix, as shown in the dashed line in Fig. 10 (a & b). For the interference studies, an antagonistic effect was observed for all anions species and concentrations listed (0.3–1000 ppm). The percent Cr(VI) removal ranged from 15 to 38% depending on the concentration and indentity of the anion. Of the anions shown in Fig. 10a, oxyanion NO_3^- tended to have the largest antagonistic effect for Cr(VI) removal especially at concentrations of 300 and 1000 ppm. This may be due to the fact that at pH 2, both the $HCrO_4$- & NO_3^- share a similar net −1 charge (please refer to speciation diagram 4c) and both involve the attraction of oxygen moieties from these oxyanions to the adsorbent. Of the anions shown in Fig. 10b, the SiO_4^{2-} created the largest depression in Cr(VI) removal at

Table 3
Comparison of the performance of the amino modified BC with various other carbonaceous adsorbent materials in term of binding capacities for Cr(VI) and Cr(III) in terms of binding capacities, as well thermodynamic information for the adsorption process.

Adsorbent	Cr(VI) binding capacity (mg/g)	Cr(III) binding capacity (mg/g)	Thermodynamics	Reference
Pine (modified)	30.49	–	Spontaneous - endothermic	https://doi.org/10.1016/j.jhazmat.2007.04.019
Almond shell	10.61	–	Nonspontaneous	https://doi.org/10.1016/S1093-0191(01)00079-X
Maple Oak tree (treated)	1.74	–	Spontaneous - endothermic	https://doi.org/10.1016/j.jhazmat.2006.06.095
Carbon-Microsilica composite	18.90	–	Nonspontaneous - exothermic	https://doi.org/10.4067/S0717-97072012000100002
Cone (Thuja oriantalis)	48.80	–	Spontaneous - endothermic	https://doi.org/10.1016/j.colsurfa.2004.10.004
GO-Fe3O4	3.20	–	Spontaneous - exothermic	https://doi.org/10.1016/j.jmrt.2020.04.040
Agave Lechuguilla Biomass	33.55	63.69	–	https://doi.org/10.1155/BCA.2005.55
Modified lignin from wood sawdust	9.30	25.00	–	https://doi.org/10.1080/009083190523352
Amino Modified Biochar	46.50	27.10	Spontaneous - exothermic	Present Study
Pine/TiO2	9.80	2.80	–	https://doi.org/10.1016/j.scitotenv.2020.143816
Pine gasification biochar	0.30	12.50	–	https://doi.org/10.1016/j.scitotenv.2020.143816
Agro-waste adsorbent	–	26.72	–	https://doi.org/10.1016/j.biortech.2010.06.020
DTPA-chitosan modified Fe3O4@SiO2	–	39.27	–	https://doi.org/10.1016/j.reactfunctpolym.2020.104720
attapulgite composite	–	10.97	Spontaneous - endothermic	https://doi.org/10.1016/j.cej.2010.12.009
chitosan/attapulgite composite	–	27.03	Spontaneous - endothermic	https://doi.org/10.1016/j.cej.2010.12.009
Thermally modified fly ash	–	2.50	Spontaneous – exothermic	https://doi.org/10.1089/ees.2016.0359

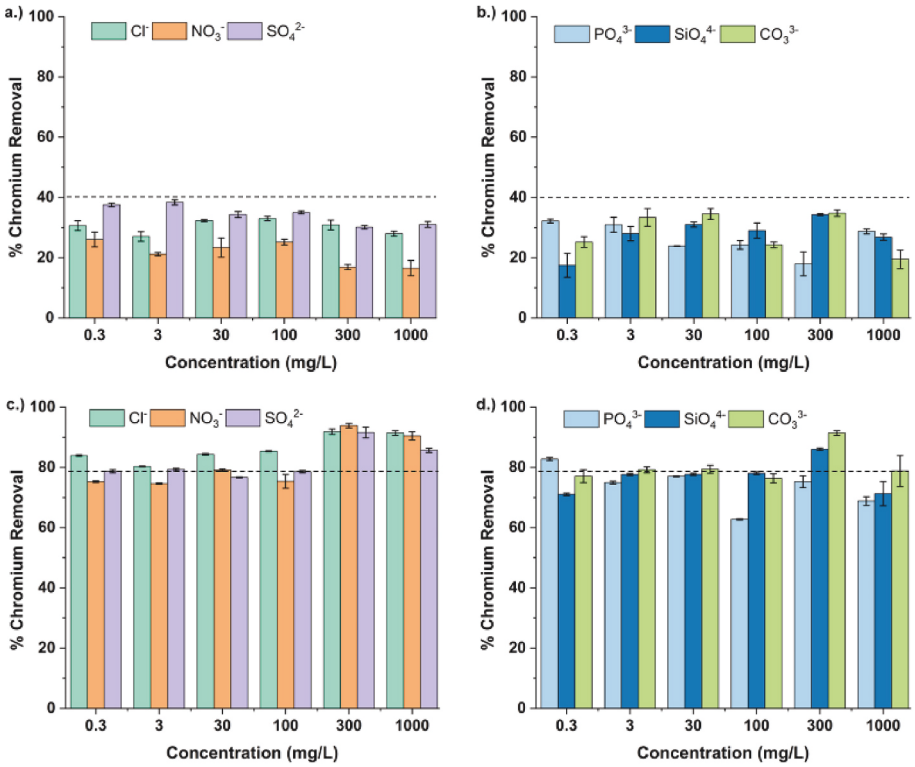

Fig. 10. Anion intereference studies for Cr(VI) adsorption on pristine BC (a & b) and Cr(VI) adsortion on the amino modified BC (c & d) expressed as % Chromium removal. Dashed line marks % Chromium Removal in ultra pure Milli-Q H_2O as benchmarking reference.

the 0.3–3.0 ppm range, while PO_4^{3-} decreased Cr(VI) removal by the greatest extent at the 30–300 ppm range. At a pH of 2, SiO_4^{2-} exists predominatley as the $H_3SiO_4^-$ species, while PO_4^{3-} exists as a mixture of $H_2PO_4^-$ and H_3PO_4 (Antonangelo et al., 2017; R.-F. Chen et al., 2021b). With such a trend in adsorption there is clear competetive effect occurring between oxyanions with similar charge and the chromate species when utilizing the pristine BC adsorbent. However, the amino modified BC was largely unaffected across all anions at all concentration ranges. As can be seen in Fig. 10c, the % Cr(VI) removal was consistent up to 100 ppm of competing anions, and a synergisitc effect on Cr(VI) adsorption was observed from 300 up to 1000 ppm of competing anions concentration. Results for the remaining anions can be seen to Fig. 10d, and were essentially unchanged for all anions at all concentrations. When compared to the results for the pristine BC, there is evident difference in level of intreference occurring in prescene of oxyanions of similar net charge. Therefore, these results further inforce the perspective that the amino modified BC is adsorbing Cr(VI) through a different mechanism (hydrogen bonding and/or complexation), rather than just pure electrostatic interaction, as observed in the pristine BC. These results show much promise for the utlization of the amino modified BC in real environmenal waters, considering that at 0.3 ppm of Cr(VI) adsorption was unaffected even at interfering anion concentrations 3,

000× that of analyte. Such selectivity for Cr(VI) over other coexisitng anions is superior to other recent reports for Cr(VI) adorbents (J. Deng et al., 2022; M. Li et al., 2022; Sahu et al., 2021; Valle et al., 2017).

The Cr(III) interference studies were performed in the prescence of common cations found in drinking water sources, which include Na^+, K^+, Ca^{2+}, and Mg^{2+} (Zachara et al., 1987). Fig. 11 below shows the results for the interference studies of pristine BC. The monovalent cations (Na^+, K^+) slightly increased Cr(III) adsorption up to 100 ppm of interfering cations, and then slightly depressed chromium % removal by approximately 15% at 1000 ppm. Conversely, the divalent cations (Ca^{2+}, Mg^{2+}) left Cr(III) adsorption unaffected at 0.3 ppm, and enhanced adsorption from 3 to 1000 ppm. With binding near 95% in higher concentrations of interfering ions, this shows excellent selectivity for Cr(III) adsortion over other common cations, upon the pristine BC adsorbent. With this increase in % Cr(III) removal, it can be hypothesized that increasing the ionic strength of the solution could be reducing the radius of the hydrated chromium ions leading to greater concentrations of adsorbed Cr(III) per adsorption site (T. Wang et al., 2013; Y. Wu et al., 2008). With the amino modified BC, monovalent cations enhanced Cr(III) adsorption to nearly 100% at all interfering ion concentrations, showing improved selectivity at higher ionic strengths. For the divalent cations Cr(III) adsorption was enhanced to nearly 100% for interfering ions concentrations at 100 ppm or lower. Above 100 ppm the binding was depressed to approximately 60% removal at 300 ppm and near 20% removal for 1000 ppm of interfering cations. As can be seen in Fig. 4d, Cr(III) exists in the $Cr(OH)^{2+}$ at a pH of 4, therefore, divalent cations displayed a greater level of competition vs the monovalent cations. In either case, with such peformace observed for both the pristine and amino modified BC materials, fantastic selectivity was mainted for % Cr(III) removal in matrices up to 100 ppm of interfering ion, which corresponds to water source of medium hardness. Thus, under hard or very hard water conditions (>300 ppm) it would appear that the pristine BC would be less susceptible to interferences when removing Cr(III) from drinking water sources (Water Science School, 2018).

4. Conclusions

Through the pyrolysis of a food waste product (pineapple skin) and green amino modification, the current work demonstrates a highly effective adsorbent material for chromium removal for polluted water sources. Through comparison of various characterization and adsorption testing it is proposed that chemical modification of the BC adsorbent resulted in reduced surface electronegativity, leading to improved interaction with the Cr(VI) containing anion. Post modification diminished N–O functionalities were observed, with new N–H and C–N bonds present. With the addition of the amino functional group, this creates further opportunity for additional adsorption mechanisms, including possible hydrogen bonding and complexation, which greatly improved the percent removal of Cr(VI) under identical conditions. The amino modification led to spontaneous Cr(VI) adsorption at all three reaction temperatures, occurring in an exothermic process. With a binding capacity of 46.5 mg/g of Cr(VI) a 10× improvement on Cr(VI) removal, and a 6× improvement on Cr(III) removal (27.1 mg/g) was observed when compared to the pristine BC. Pristine BC showed an exothermic trend for Cr(VI) adsorption and endothermic for Cr(III), while the amino modified BC expressed a complete exothermic process for both ions. In addition, the pristine BC was observed to bind spontaneously to Cr(III), while both Cr(VI) and Cr(III) binding to the amino modified was spontaneous at room temperature. SEM-EDS revealed that Cr(VI) adsorption occurred in areas of high nitrogen atom concentrations, suggesting enhanced coordination at these sites.

Regarding performance of the adsorbents in real matrices, interference studies revealed excellent selectivity for Cr(VI) adsorption upon the amino modified adsorbent, and selective adsorption of Cr(III) in both adsorbents. Pristine BC was significantly impacted by the presence of competing anions for the adsorption of Cr(VI). Conversely, the amino modified BC was unaffected in solutions up to 100 ppm of interfering anions, and synergized increasing removal performance (>90%) at 300 & 1000 ppm. This performance was favorable considering that Cr(VI) was present at 0.3 ppm, within interfering anions nearly 3,000× more concentrated. For the pristine BC Cr(III) % removal was largely unaffected at all tested interfering cation concentrations, showing much promise for real world applications. Whereas, Cr(III) adsorption upon the amino modified BC was synergized to nearly 100% removal when cations interfering solutions had concentrations of up to 100 ppm, and the binding was suppressed thereafter for divalent cations. With such performance it can be seen that the amino modified BC should perform excellently for Cr(VI) removal, even in highly complex matrices, as well as for Cr(III) contained in moderately hard waters. While the amino modified BC has showed cased excellent selective remediation for both Cr ions, further testing should be geared towards implementing in this material into stationary supports or membranes in order to heighten this materials probability for upscaled water treatment applications.

CRediT authorship contribution statement

Kenneth Flores: Writing – review & editing, Writing – original draft, Visualization, Validation, Methodology, Investigation, Formal analysis, Conceptualization. **Diego F. Gonzalez:** Validation, Methodology, Investigation, Formal analysis. **Helia M. Morales:** Validation, Methodology, Investigation. **Arnulfo Mar:** Writing – review & editing, Formal analysis. **Sergi Garcia-Segura:** Writing – review & editing, Validation, Formal analysis. **Jorge L. Gardea-Torresdey:** Writing – review & editing, Validation, Formal analysis. **Jason G. Parsons:** Writing – review & editing, Validation, Supervision, Resources, Project administration, Methodology, Funding acquisition, Formal analysis, Conceptualization.

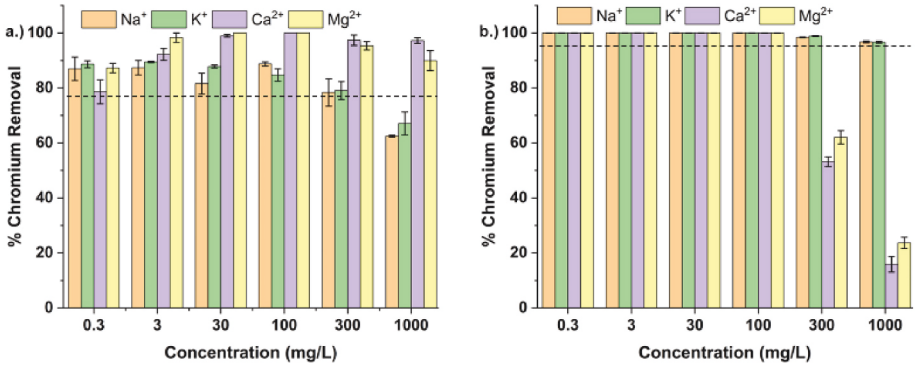

Fig. 11. Cation interference studies for Cr(III) adsorption upon the pristine BC (a.), amino modified BC (b.), cation and anions combination interfernce results for pristine BC. Dashed line marks % Chromium Removal in ultra pure Milli Q H_2O.

Declaration of competing interest

The authors declare that they have no known competing financial interests or personal relationships that could have appeared to influence the work reported in this paper.

Data availability

Data will be made available on request.

Acknowledgements

K.F acknowledges, this material is based upon work supported by the National Science Foundation MPS-Ascend Postdoctoral Research Fellowship under Grant No. 2316072. **J.L.G.T.** acknowledges partial funding provided by the NSF ERC on Nanotechnology-Enabled Water Treatment (EEC-1449500), the Dudley family for the Endowed Research Professorship and the University of Texas System's 2018 STARs Retention Award, USDA-NIFA # 2023-67021-39747, and NSF MRI Grant No. 2216473. **J.G.P.** acknowledges and is grateful for the support provided by funding from the UTRGV Chemistry Departmental Welch Foundation Grant (Grant No: BX-0048).

References

Akram, M., Bhatti, H.N., Iqbal, M., Noreen, S., Sadaf, S., 2017. Biocomposite efficiency for Cr(VI) adsorption: kinetic, equilibrium and thermodynamics studies. J. Environ. Chem. Eng. 5 (1), 400–411. https://doi.org/10.1016/j.jece.2016.12.002.

Alcamo, J., Henrichs, T., Rosch, T., 2000. World Water in 2025.Pdf (World Water Series Report. University of Kassel, pp. 1–49. http://www.env-edu.gr/Documents/World%20Water%20in%202025.pdf.

Antonangelo, J.A., Ferrari Neto, J., Crusciol, C.A.C., Alleoni, L.R.F., 2017. Lime and calcium-magnesium silicate in the ionic speciation of an Oxisol. Sci. Agric. 74 (4), 317–333. https://doi.org/10.1590/1678-992x-2016-0372.

Auta, M., Hameed, B.H., 2012. Modified mesoporous clay adsorbent for adsorption isotherm and kinetics of methylene blue. Chem. Eng. J. 198–199, 219–227. https://doi.org/10.1016/j.cej.2012.05.075.

Babapour, M., Hadi Dehghani, M., Alimohammadi, M., Moghadam Arjmand, M., Salari, M., Rasuli, L., Mubarak, N.M., Ahmad Khan, N., 2022. Adsorption of Cr(VI) from aqueous solution using mesoporous metal-organic framework-5 functionalized with the amino acids: characterization, optimization, linear and nonlinear kinetic models. J. Mol. Liq. 345, 117835 https://doi.org/10.1016/j.molliq.2021.117835.

Babu, B.V., Gupta, S., 2008. Adsorption of Cr(VI) using activated neem leaves: kinetic studies. Adsorption 14 (1), 85–92. https://doi.org/10.1007/s10450-007-9057-x.

Baby, R., Saifullah, B., Hussein, M.Z., 2019. Carbon nanomaterials for the treatment of heavy metal-contaminated water and environmental remediation. Nanoscale Res. Lett. 14 (1), 341. https://doi.org/10.1186/s11671-019-3167-8.

Bai, C., Wang, L., Zhu, Z., 2020. Adsorption of Cr(III) and Pb(II) by graphene oxide/alginate hydrogel membrane: characterization, adsorption kinetics, isotherm and thermodynamics studies. Int. J. Biol. Macromol. 147, 898–910. https://doi.org/10.1016/j.ijbiomac.2019.09.249.

Blanchard, G., Maunaye, M., Martin, G., 1984. Removal of heavy metals from waters by means of natural zeolites. Water Res. 18 (12), 1501–1507. https://doi.org/10.1016/0043-1354(84)90124-6.

Brewer, C.E., Chuang, V.J., Masiello, C.A., Gonnermann, H., Gao, X., Dugan, B., Driver, L. E., Panzacchi, P., Zygourakis, K., Davies, C.A., 2014. New approaches to measuring biochar density and porosity. Biomass Bioenergy 66, 176–185. https://doi.org/10.1016/j.biombioe.2014.03.059.

Cantu, Y., Remes, A., Reyna, A., Martinez, D., Villarreal, J., Ramos, H., Trevino, S., Tamez, C., Martinez, A., Eubanks, T., Parsons, J.G., 2014. Thermodynamics, kinetics, and activation energy studies of the sorption of chromium(III) and chromium(VI) to a Mn3O4 nanomaterial. Chem. Eng. J. 254, 374–383. https://doi.org/10.1016/j.cej.2014.05.110.

Chen, N., Cao, S., Zhang, L., Peng, X., Wang, X., Ai, Z., Zhang, L., 2021a. Structural dependent Cr(VI) adsorption and reduction of biochar: hydrochar versus pyrochar. Sci. Total Environ. 783, 147084 https://doi.org/10.1016/j.scitotenv.2021.147084.

Chen, R.-F., Liu, T., Rong, H.-W., Zhong, H.-T., Wei, C.-H., 2021b. Effect of organic substances on nutrients recovery by struvite electrochemical precipitation from synthetic anaerobically treated swine wastewater. Membranes 11 (8), 594. https://doi.org/10.3390/membranes11080594.

Chen, S., Yue, Q., Gao, B., Li, Q., Xu, X., 2011. Removal of Cr(VI) from aqueous solution using modified corn stalks: characteristic, equilibrium, kinetic and thermodynamic study. Chem. Eng. J. 168 (2), 909–917. https://doi.org/10.1016/j.cej.2011.01.063.

Chen, W., Shi, S., Nguyen, T., Chen, M., Zhou, X., 2016. Effect of temperature on the evolution of physical structure and chemical properties of bio-char derived from Co-pyrolysis of lignin with high-density polyethylene. Bioresources 11 (2), 3923–3936. https://doi.org/10.15376/biores.11.2.3923-3936.

Chen, X., Hossain, M.F., Duan, C., Lu, J., Tsang, Y.F., Islam, M.S., Zhou, Y., 2022. Isotherm models for adsorption of heavy metals from water—a review. Chemosphere 307, 135545. https://doi.org/10.1016/j.chemosphere.2022.135545.

Cho, D.-W., Chon, C.-M., Kim, Y., Jeon, B.-H., Schwartz, F.W., Lee, E.-S., Song, H., 2011. Adsorption of nitrate and Cr(VI) by cationic polymer-modified granular activated carbon. Chem. Eng. J. 175, 298–305. https://doi.org/10.1016/j.cej.2011.09.108.

Dehouli, H., Chedeville, O., Cagnon, B., Caqueret, V., Porte, C., 2010. Influences of pH, temperature and activated carbon properties on the interaction ozone/activated carbon for a wastewater treatment process. Desalination 254 (1–3), 12–16. https://doi.org/10.1016/j.desal.2009.12.021.

Deng, J., Liu, Y., Li, H., Huang, Z., Qin, X., Huang, J., Zhang, X., Li, X., Lu, Q., 2022. A novel biochar-copolymer composite for rapid Cr(VI) removal: adsorption-reduction performance and mechanism. Separ. Purif. Technol. 295, 121275 https://doi.org/10.1016/j.seppur.2022.121275.

Deng, S., Bai, R., 2004. Removal of trivalent and hexavalent chromium with aminated polyacrylonitrile fibers: performance and mechanisms. Water Res. 38 (9), 2424–2432. https://doi.org/10.1016/j.watres.2004.02.024.

Efficient Removal of Cr(VI) from Aqueous Solution onto Palm Trunk Charcoal: Kinetic and Equilibrium Studies, 2016. Chem. Sci. J. https://doi.org/10.4172/2150-3494.1000114.

Ekanayake, A., Rajapaksha, A.U., Selvasembian, R., Vithanage, M., 2022. Amino-functionalized biochars for the detoxification and removal of hexavalent chromium in aqueous media. Environ. Res. 211, 113073 https://doi.org/10.1016/j.envres.2022.113073.

Elnour, A.Y., Alghyamah, A.A., Shaikh, H.M., Poulose, A.M., Al-Zahrani, S.M., Anis, A., Al-Wabel, M.I., 2019. Effect of pyrolysis temperature on biochar microstructural evolution, physicochemical characteristics, and its influence on biochar/polypropylene composites. Appl. Sci. 9 (6), 1149. https://doi.org/10.3390/app9061149.

Fang, L., Huang, T., Lu, H., Wu, X.-L., Chen, Z., Yang, H., Wang, S., Tang, Z., Li, Z., Hu, B., Wang, X., 2023. Biochar-based materials in environmental pollutant elimination, H2 production and CO2 capture applications. Biochar 5 (1), 42. https://doi.org/10.1007/s42773-023-00237-7.

Guo, C., Zou, J., Yang, J., Wang, K., Song, S., 2020. Surface characterization of maize-straw-derived biochar and their sorption mechanism for Pb2+ and methylene blue. PLoS One 15 (8), e0238105. https://doi.org/10.1371/journal.pone.0238105.

Gupta, V.K., Carrott, P.J.M., Ribeiro Carrott, M.M.L., Suhas, 2009. Low-Cost adsorbents: growing approach to wastewater treatment—a review. Crit. Rev. Environ. Sci. Technol. 39 (10), 783–842. https://doi.org/10.1080/10643380801977610.

Han, X., Wong, Y.S., Tam, N.F.Y., 2006. Surface complexation mechanism and modeling in Cr(III) biosorption by a microalgal isolate, Chlorella miniata. J. Colloid Interface Sci. 303 (2), 365–371. https://doi.org/10.1016/j.jcis.2006.08.028.

Hautman, D., Munch, D., Pfaff, J., 1999. METHOD 300.1, DETERMINATION OF INORGANIC ANIONS IN DRINKING WATER BY ION CHROMATOGRAPHY. United States Environmental Protection Agency, pp. 1–40 [U.S Goverment Report]. https://www.epa.gov/sites/default/files/2015-06/documents/epa-300.1.pdf.

Ho, Y.S., McKay, G., 1998. Sorption of dye from aqueous solution by peat. Chem. Eng. J. 70 (2), 115–124. https://doi.org/10.1016/S0923-0467(98)00076-1.

Hui, M., Shengyan, P., Yaqi, H., Rongxin, Z., Anatoly, Z., Wei, C., 2018. A highly efficient magnetic chitosan "fluid" adsorbent with a high capacity and fast adsorption kinetics for dyeing wastewater purification. Chem. Eng. J. 345, 556–565. https://doi.org/10.1016/j.cej.2018.03.115.

Infrared Spectroscopy Absorption Table, 2020. LibreTexts Chemistry [Spectroscopic Reference Table]. https://chem.libretexts.org/Ancillary_Materials/Reference/Reference_Tables/Spectroscopic_Reference_Tables/Infrared_Spectroscopy_Absorption_Table.

IR Spectrum Table & Chart, 2023. Millipore Sigma. https://www.sigmaaldrich.com/US/en/technical-documents/technical-article/analytical-chemistry/photometry-and-reflectometry/ir-spectrum-table.

Jin, X., Liu, R., Wang, H., Han, L., Qiu, M., Hu, B., 2022. Functionalized porous nanoscale Fe3O4 particles supported biochar from peanut shell for Pb(II) ions removal from landscape wastewater. Environ. Sci. Pollut. Control Ser. 29 (25), 37159–37169. https://doi.org/10.1007/s11356-021-18432-z.

Keiluweit, M., Nico, P.S., Johnson, M.G., Kleber, M., 2010. Dynamic molecular structure of plant biomass-derived black carbon (biochar). Environ. Sci. Technol. 44 (4), 1247–1253. https://doi.org/10.1021/es9031419.

Kenfoud, H., Nasrallah, N., Baaloudj, O., Derridj, F., Trari, M., 2022. Enhanced photocatalytic reduction of Cr(VI) by the novel hetero-system BaFe2O4/SnO2. J. Phys. Chem. Solid. 160, 110315 https://doi.org/10.1016/j.jpcs.2021.110315.

Kołodyńska, D., Wnętrzak, R., Leahy, J.J., Hayes, M.H.B., Kwapiński, W., Hubicki, Z., 2012. Kinetic and adsorptive characterization of biochar in metal ions removal. Chem. Eng. J. 197, 295–305. https://doi.org/10.1016/j.cej.2012.05.025.

Kosmulski, M., 2011. The pH-dependent surface charging and points of zero charge. J. Colloid Interface Sci. 353 (1), 1–15. https://doi.org/10.1016/j.jcis.2010.08.023.

Ksakas, A., Loqman, A., El Bali, B., Taleb, M., Kherbeche, A., 2015. The adsorption of Cr (VI) from aqueous solution by natural materials. J. Mater. Environ. Sci. 6 (7), 2003–2012.

Kumar, V., Leekha, A., Tyagi, A., Kaul, A., Mishra, A.K., Verma, A.K., 2017. Preparation and evaluation of biopolymeric nanoparticles as drug delivery system in effective treatment of rheumatoid arthritis. Pharmaceut. Res. 34 (3), 654–667. https://doi.org/10.1007/s11095-016-2094-y.

Le, C., Wu, J.H., Deng, S.B., Li, P., Wang, X.D., Zhu, N.W., Wu, P.X., 2011. Effects of common dissolved anions on the reduction of para-chloronitrobenzene by zero-valent iron in groundwater. Water Sci. Technol. 63 (7), 1485–1490. https://doi.org/10.2166/wst.2011.392.

Li, M., Tang, C., Fu, S., Tam, K.C., Zong, Y., 2022. Cellulose-based aerogel beads for efficient adsorption- reduction- sequestration of Cr(VI). Int. J. Biol. Macromol. 216, 860–870. https://doi.org/10.1016/j.ijbiomac.2022.07.215.

Li, Q., Yue, Q.-Y., Su, Y., Gao, B.-Y., Sun, H.-J., 2010. Equilibrium, thermodynamics and process design to minimize adsorbent amount for the adsorption of acid dyes onto cationic polymer-loaded bentonite. Chem. Eng. J. 158 (3), 489–497. https://doi.org/10.1016/j.cej.2010.01.033.

Li, Q., Zhu, Y., Zhao, P., Yuan, C., Chen, M., Wang, C., 2018. Commercial activated carbon as a novel precursor of the amorphous carbon for high-performance sodium-ion batteries anode. Carbon 129, 85–94. https://doi.org/10.1016/j.carbon.2017.12.008.

Li, Y., Yu, H., Liu, L., Yu, H., 2021. Application of co-pyrolysis biochar for the adsorption and immobilization of heavy metals in contaminated environmental substrates. J. Hazard Mater. 420, 126655 https://doi.org/10.1016/j.jhazmat.2021.126655.

Liang, L., Xi, F., Tan, W., Meng, X., Hu, B., Wang, X., 2021. Review of organic and inorganic pollutants removal by biochar and biochar-based composites. Biochar 3 (3), 255–281. https://doi.org/10.1007/s42773-021-00101-6.

Liu, F., Hua, S., Wang, C., Qiu, M., Jin, L., Hu, B., 2021a. Adsorption and reduction of Cr (VI) from aqueous solution using cost-effective caffeic acid functionalized corn starch. Chemosphere 279, 130539. https://doi.org/10.1016/j.chemosphere.2021.130539.

Liu, F., Lou, Y., Xia, F., Hu, B., 2023a. Immobilizing nZVI particles on MBenes to enhance the removal of U(VI) and Cr(VI) by adsorption-reduction synergistic effect. Chem. Eng. J. 454, 140318 https://doi.org/10.1016/j.cej.2022.140318.

Liu, F., Wang, S., Hu, B., 2023b. Electrostatic self-assembly of nanoscale FeS onto MXenes with enhanced reductive immobilization capability for U(VI) and Cr(VI). Chem. Eng. J. 456, 141100 https://doi.org/10.1016/j.cej.2022.141100.

Liu, F., Wang, S., Zhao, C., Hu, B., 2023c. Constructing coconut shell biochar/MXenes composites through self-assembly strategy to enhance U(VI) and Cs(I) immobilization capability. Biochar 5 (1), 31. https://doi.org/10.1007/s42773-023-00231-z.

Liu, H., Zhang, S., Yang, J., Ji, M., Yu, J., Wang, M., Chai, X., Yang, B., Zhu, C., Xu, J., 2019. Preparation, stabilization and carbonization of a novel polyacrylonitrile-based carbon fiber precursor. Polymers 11 (7), 1150. https://doi.org/10.3390/polym11071150.

Liu, R., Wang, H., Han, L., Hu, B., Qiu, M., 2021b. Reductive and adsorptive elimination of U(VI) ions in aqueous solution by SFeS@Biochar composites. Environ. Sci. Pollut. Control Ser. 28 (39), 55176–55185. https://doi.org/10.1007/s11356-021-14835-0.

Liu, Y., Zhao, X., Li, J., Ma, D., Han, R., 2012. Characterization of bio-char from pyrolysis of wheat straw and its evaluation on methylene blue adsorption. Desalination Water Treat. 46 (1–3), 115–123. https://doi.org/10.1080/19443994.2012.677408.

Lu, Y., Cai, Y., Zhang, S., Zhuang, L., Hu, B., Wang, S., Chen, J., Wang, X., 2022. Application of biochar-based photocatalysts for adsorption-(photo)degradation/reduction of environmental contaminants: mechanism, challenges and perspective. Biochar 4 (1), 45. https://doi.org/10.1007/s42773-022-00173-y.

Mallik, A.K., Moktadir, Md A., Rahman, Md A., Shahruzzaman, Md, Rahman, M.M., 2022. Progress in surface-modified silicas for Cr(VI) adsorption: a review. J. Hazard Mater. 423, 127041 https://doi.org/10.1016/j.jhazmat.2021.127041.

Mariana, M., Khalil, A., Mistar, E.M., Yahya, E.B., Alfatah, T., Danish, M., Amayreh, M., 2021. Recent advances in activated carbon modification techniques for enhanced heavy metal adsorption. J. Water Proc. Eng. 43, 102221. https://doi.org/10.1016/j.jwpe.2021.102221.

Miretzky, P., Cirelli, A.F., 2010. Cr(VI) and Cr(III) removal from aqueous solution by raw and modified lignocellulosic materials: a review. J. Hazard Mater. 180 (1–3), 1–19. https://doi.org/10.1016/j.jhazmat.2010.04.060.

Nkuigue Fotsing, P., Bouazizi, N., Djoufac Woumfo, E., Mofaddel, N., Le Derf, F., Vieillard, J., 2021. Investigation of chromate and nitrate removal by adsorption at the surface of an amine-modified cocoa shell adsorbent. J. Environ. Chem. Eng. 9 (1), 104618 https://doi.org/10.1016/j.jece.2020.104618.

Nur-E-Alam, Md, Mia, Md A.S., Ahmad, F., Rahman, Md M., 2020. An overview of chromium removal techniques from tannery effluent. Appl. Water Sci. 10 (9), 205. https://doi.org/10.1007/s13201-020-01286-0.

Park, S., Baker, J.O., Himmel, M.E., Parilla, P.A., Johnson, D.K., 2010. Cellulose crystallinity index: measurement techniques and their impact on interpreting cellulase performance. Biotechnol. Biofuels 3 (1), 10. https://doi.org/10.1186/1754-6834-3-10.

Parsons, J.G., Hejazi, M., Tiemann, K.J., Henning, J., Gardea-Torresdey, J.L., 2002. An XAS study of the binding of copper(II), zinc(II), chromium(III) and chromium(VI) to hops biomass. Microchem. J. 71 (2–3), 211–219. https://doi.org/10.1016/S0026-265X(02)00013-9.

Partlan, E., Ren, Y., Apul, O.G., Ladner, D.A., Karanfil, T., 2020. Adsorption kinetics of synthetic organic contaminants onto superfine powdered activated carbon. Chemosphere 253, 126628. https://doi.org/10.1016/j.chemosphere.2020.126628.

Qiu, M., Liu, L., Ling, Q., Cai, Y., Yu, S., Wang, S., Fu, D., Hu, B., Wang, X., 2022. Biochar for the removal of contaminants from soil and water: a review. Biochar 4 (1), 19. https://doi.org/10.1007/s42773-022-00146-1.

Quan, Y., Liu, Q., Zhang, S., Zhang, S., 2018. Comparison of the morphology, chemical composition and microstructure of cryptocrystalline graphite and carbon black. Appl. Surf. Sci. 445, 335–341. https://doi.org/10.1016/j.apsusc.2018.03.182.

Ryu, S.R., Noda, I., Jung, Y.M., 2010. What is the origin of positional fluctuation of spectral features: true frequency shift or relative intensity changes of two overlapped bands? Appl. Spectrosc. 64 (9), 1017–1021. https://doi.org/10.1366/000370210792434396.

Saha, P., Chowdhury, S., 2011. Insight into Adsorption Thermodynamics—Chapter 16. IntechOpen.

Sahu, S., Bishoyi, N., Sahu, M.K., Patel, R.K., 2021. Investigating the selectivity and interference behavior for detoxification of Cr(VI) using lanthanum phosphate polyaniline nanocomposite via adsorption-reduction mechanism. Chemosphere 278, 130507. https://doi.org/10.1016/j.chemosphere.2021.130507.

Selomulya, C., Meeyoo, V., Amal, R., 1999. Mechanisms of Cr(VI) removal from water by various types of activated carbons. J. Chem. Technol. Biotechnol. 74 (2), 111–122. https://doi.org/10.1002/(SICI)1097-4660(199902)74:2<111::AID-JCTB990>3.0.CO;2-D.

Sharma, P., Singh, S.P., Parakh, S.K., Tong, Y.W., 2022. Health hazards of hexavalent chromium (Cr (VI)) and its microbial reduction. Bioengineered 13 (3), 4923–4938. https://doi.org/10.1080/21655979.2022.2037273.

Silber, A., Levkovitch, I., Graber, E.R., 2010. pH-dependent mineral release and surface properties of cornstraw biochar: agronomic implications. Environ. Sci. Technol. 44 (24), 9318–9323. https://doi.org/10.1021/es101283d.

Togue Kamga, F., 2019. Modeling adsorption mechanism of paraquat onto Ayous (Triplochiton scleroxylon) wood sawdust. Appl. Water Sci. 9 (1), 1. https://doi.org/10.1007/s13201-018-0879-3.

Tumolo, M., Ancona, V., De Paola, D., Losacco, D., Campanale, C., Massarelli, C., Uricchio, V.F., 2020a. Chromium pollution in European water, sources, health risk, and remediation strategies: an overview. Int. J. Environ. Res. Publ. Health 17 (15), 5438. https://doi.org/10.3390/ijerph17155438.

Tumolo, M., Ancona, V., De Paola, D., Losacco, D., Campanale, C., Massarelli, C., Uricchio, V.F., 2020b. Chromium pollution in European water, sources, health risk, and remediation strategies: an overview. Int. J. Environ. Res. Publ. Health 17 (15), 5438. https://doi.org/10.3390/ijerph17155438.

Valle, J.P., Gonzalez, B., Schulz, J., Salinas, D., Romero, U., Gonzalez, D.F., Valdes, C., Cantu, J.M., Eubanks, T.M., Parsons, J.G., 2017. Sorption of Cr(III) and Cr(VI) to K 2 Mn 4 O 9 nanomaterial a study of the effect of pH, time, temperature and interferences. Microchem. J. 133, 614–621. https://doi.org/10.1016/j.microc.2017.04.021.

Varadharajan, C., Beller, H.R., Bill, M., Brodie, E.L., Conrad, M.E., Han, R., Irwin, C., Larsen, J.T., Lim, H.-C., Molins, S., Steefel, C.I., Van Hise, A., Yang, L., Nico, P.S., 2017. Reoxidation of chromium(III) products formed under different biogeochemical regimes. Environ. Sci. Technol. 51 (9), 4918–4927. https://doi.org/10.1021/acs.est.6b06044.

Wang, C., Gu, L., Liu, X., Zhang, X., Cao, L., Hu, X., 2016. Sorption behavior of Cr(VI) on pineapple-peel-derived biochar and the influence of coexisting pyrene. Int. Biodeterior. Biodegrad. 111, 78–84. https://doi.org/10.1016/j.ibiod.2016.04.029.

Wang, J., Guo, X., 2020. Adsorption kinetic models: physical meanings, applications, and solving methods. J. Hazard Mater. 390, 122156 https://doi.org/10.1016/j.jhazmat.2020.122156.

Wang, T., Liu, W., Xiong, L., Xu, N., Ni, J., 2013. Influence of pH, ionic strength and humic acid on competitive adsorption of Pb(II), Cd(II) and Cr(III) onto titanate nanotubes. Chem. Eng. J. 215–216, 366–374. https://doi.org/10.1016/j.cej.2012.11.029.

Water Science School, 2018. Hardness of Water. United States Geological Survey. https://www.usgs.gov/special-topics/water-science-school/science/hardness-water#:~:text=Measures%20of%20water%20hardness&text=General%20guidelines%20for%20classification%20of,mg%2FL%20as%20very%20hard.

Weber, W.J., Morris, J.C., 1963. Kinetics of adsorption on carbon from solution. J. Sanit. Eng. Div. 89 (2), 31–59. https://doi.org/10.1061/JSEDAI.0000430.

Wu, J., Wang, T., Shi, N., Pan, W.-P., 2022. Insight into mass transfer mechanism and equilibrium modeling of heavy metals adsorption on hierarchically porous biochar. Separ. Purif. Technol. 287, 120558 https://doi.org/10.1016/j.seppur.2022.120558.

Wu, Y., Zhang, S., Guo, X., Huang, H., 2008. Adsorption of chromium(III) on lignin. Bioresour. Technol. 99 (16), 7709–7715. https://doi.org/10.1016/j.biortech.2008.01.069.

Yang, G.-X., Jiang, H., 2014. Amino modification of biochar for enhanced adsorption of copper ions from synthetic wastewater. Water Res. 48, 396–405. https://doi.org/10.1016/j.watres.2013.09.050.

Yang, S., Li, L., Pei, Z., Li, C., Lv, J., Xie, J., Wen, B., Zhang, S., 2014. Adsorption kinetics, isotherms and thermodynamics of Cr(III) on graphene oxide. Colloids Surf. A Physicochem. Eng. Asp. 457, 100–106. https://doi.org/10.1016/j.colsurfa.2014.05.062.

Yoo, S., Kelley, S.S., Tilotta, D.C., Park, S., 2018. Structural characterization of loblolly pine derived biochar by X-ray diffraction and electron energy loss spectroscopy. ACS Sustain. Chem. Eng. 6 (2), 2621–2629. https://doi.org/10.1021/acssuschemeng.7b04119.

Zachara, J.M., Girvin, D.C., Schmidt, R.L., Resch, C. Thomas, 1987. Chromate adsorption on amorphous iron oxyhydroxide in the presence of major groundwater ions. Environ. Sci. Technol. 21 (6), 589–594. https://doi.org/10.1021/es00160a010.

Zaheer, Z., AbuBaker Bawazir, W., Al-Bukhari, S.M., Basaleh, A.S., 2019. Adsorption, equilibrium isotherm, and thermodynamic studies to the removal of acid orange 7. Mater. Chem. Phys. 232, 109–120. https://doi.org/10.1016/j.matchemphys.2019.04.064.

Zheng, C., Yang, Z., Si, M., Zhu, F., Yang, W., Zhao, F., Shi, Y., 2021. Application of biochars in the remediation of chromium contamination: fabrication, mechanisms, and interfering species. J. Hazard Mater. 407, 124376 https://doi.org/10.1016/j.jhazmat.2020.124376.

Zhitkovich, A., 2011. Chromium in drinking water: sources, metabolism, and cancer risks. Chem. Res. Toxicol. 24 (10), 1617–1629. https://doi.org/10.1021/tx200251t.

Zhou, S., Mo, X., Zhu, W., Xu, W., Tang, K., Lei, Y., 2020. Selective adsorption of Au(III) with ultra-fast kinetics by a new metal-organic polymer. J. Mol. Liq. 319, 114125 https://doi.org/10.1016/j.molliq.2020.114125.